Journal of Diabetes Science and Technology
Volume 6, Issue 6, November 2012

ORIGINAL ARTICLE

Continuous Monitoring of Glucose in Subcutaneous Tissue Using Microfabricated Differential Affinity Sensors

Xian Huang, Ph.D.,[1] Charles Leduc, Ph.D.,[2] Yann Ravussin, Ph.D.,[2] Siqi Li, Ph.D.,[3] Erin Davis, M.S.,[3] Bing Song, M.S.,[1] Qian Wang, Ph.D.,[3] Domenico Accili, M.D.,[2] Rudolph Leibel, M.D.,[2] and Qiao Lin, Ph.D.[1]

Abstract

Objective:

We describe miniaturized differential glucose sensors based on affinity binding between glucose and a synthetic polymer. The sensors possess excellent resistance to environmental disturbances and can potentially allow wireless measurements of glucose concentrations within interstitial fluid in subcutaneous tissue for long-term, stable continuous glucose monitoring (CGM).

Methods:

The sensors are constructed using microelectromechanical systems (MEMS) technology and exploit poly(N-hydroxyethyl acrylamide-*ran*-3-acrylamidophenylboronic acid) (PHEAA-*ran*-PAAPBA), a glucose-binding polymer with excellent specificity, reversibility, and stability. Two sensing approaches have been investigated, which respectively, use a pair of magnetically actuated diaphragms and perforated electrodes to differentially measure the glucose-binding-induced changes in the viscosity and permittivity of the PHEAA-*ran*-PAAPBA solution with respect to a reference, glucose-unresponsive polymer solution.

Results:

In vivo characterization of the MEMS affinity sensors were performed by controlling blood glucose concentrations of laboratory mice by exogenous glucose and insulin administration. The sensors experienced an 8–30 min initialization period after implantation and then closely tracked commercial capillary glucose meter readings with time lags ranging from 0–15 min during rapid glucose concentration changes. Clarke error grid plots obtained from sensor calibration suggest that, for the viscometric and dielectric sensors, respectively, approximately 95% (in the hyperglycemic range) and 84% (ranging from hypoglycemic to hyperglycemic glucose concentrations) of measurement points were clinically accurate, while 5% and 16% of the points were clinically acceptable.

continued →

Author Affiliations: [1]Department of Mechanical Engineering, Columbia University, New York, New York; [2]Department of Pediatrics, Columbia University Medical Center, New York, New York; and [3]Department of Chemistry and Biochemistry, University of South Carolina, Columbia, South Carolina

Abbreviations: (AC) alternating current, (CGM) continuous glucose monitoring, (IP) intraperitoneal, (ISF) interstitial fluid, (MEMS) microelectromechanical systems, (PAA) poly(acrylamide), (PAAPBA) poly(acrylamidophenylboronic acid), (PBS) phosphate-buffered saline, (PHEAA) poly(N-hydroxyethyl acrylamide), (PHEAA-*ran*-PAAPBA) poly(N-hydroxyethyl acrylamide-ran-3-acrylamidophenylboronic acid)

Keywords: animal experiment, capacitive detection, continuous glucose monitoring, dielectric sensor, differential measurement, viscometric sensor

Corresponding Author: Xian Huang, Ph.D., Department of Mechanical Engineering, Columbia University, 220 S. W. Mudd, 500 W. 120th St., New York, NY 10027; email address xh2123@columbia.edu

Abstract cont.

Conclusions:

The miniaturized MEMS sensors explore differential measurements of affinity glucose recognition. *In vivo* testing demonstrated excellent accuracy and stability, suggesting that the devices hold the potential to enable long-term and reliable CGM in clinical applications.

J Diabetes Sci Technol 2012;6(6):1436-1444

Introduction

Glucose monitoring for diabetes care is typically performed by serial finger stick testing,[1] which is uncomfortable, distracting, and can potentially miss abnormal blood sugar excursions during sleep, after insulin administration, or following meals. Continuous glucose monitoring (CGM), which measures glucose in a virtually continuous manner throughout the day and night, is an emerging technique for more effective blood sugar management. Currently, CGM is commonly realized via subcutaneously implanted glucose sensors that detect glucose concentrations in interstitial fluid (ISF) through enzymatic electrochemical reactions.[2–4] Such electrochemical CGM sensors typically have limited stability and longevity due to issues such as irreversible glucose consumption,[5] erosion of sensor electrodes, degradation of functional enzymes,[6] and interference by electrode-active chemicals. In addition, biofouling, or deposition of biological material on sensor surfaces, can also hinder the transport of glucose to functional enzymes, resulting in oxygen deficit at the electrodes,[7] which significantly affects their accuracy and reliability. In contrast, glucose affinity sensing based on equilibrium binding between glucose and its specific receptors offers an attractive alternative to CGM applications.[8,9] These methods are nonconsumptive, eliminating sensor-induced changes in local glucose concentrations and generation of potentially interfering reaction products. Moreover, affinity sensing is more tolerant of biofouling, as the accumulation of biological materials on the implanted sensor surface only influences the time to achieve equilibrium binding rather than measurement accuracy.

Miniaturized affinity glucose sensors enabled by microelectromechanical systems (MEMS) technology can offer significant advantages, such as improved measurement time response, minimal invasiveness, and enhanced reliability. Existing MEMS affinity glucose sensors measure glucose-induced changes in fluorescence intensity,[9,10] viscosity,[11–13] osmotic pressure,[14] conductivity,[15] and permittivity[16] of the recognition material. In addition, MEMS devices that have been demonstrated to sample blood or ISF by microdialysis,[17,18] microneedle–skin interfacing,[19] sohophoresis,[20] and microablation[21] can be combined with affinity sensing for epidermal glucose detection. We have previously reported MEMS affinity glucose sensors that measured the glucose-induced changes in the viscosity and permittivity of polymer solutions.[12,16] Using a synthetic polymer for glucose recognition, these devices effectively address aforementioned issues of electrochemical sensors and have demonstrated specific, reversible, and stable glucose detection at physiologically relevant pH values. However, these sensors contain only a single glucose-detecting module without allowing for the effects of environmental disturbances such as temperature variations and human activity. As such, they are not yet appropriate for *in vivo* applications.

In this article, we describe MEMS differential affinity glucose sensors based on viscometric and dielectric detection. These differential sensors consist of a glucose-responsive sensing module and a glucose-unresponsive reference module. The sensing module is integrated with a synthetic affinity polymer solution that provides highly specific glucose-binding and possesses long-term stability, while the properties of the reference module only change in response to environmental fluctuations.[22,23] The sensors determine glucose concentrations by viscosity or permittivity differences between the two modules by differential capacitance detection, which effectively rejects common mode disturbances and yields improved stability and reliability in implantable measurements by an implanted device. Results from preliminary animal testing by implanting sensors subcutaneously in laboratory mice show the potential of the devices for stable and reliable CGM.

Materials and Methods

Principle and Design

The MEMS differential affinity glucose sensors consist of a glucose-sensing module and a reference module placed in close proximity to each other (**Figure 1**). The modules each comprise a microchamber, referred to as the sensing microchamber, and a reference chamber, respectively. The chambers each house a surface-machined transducing element and are equipped with a semi-permeable membrane that allows glucose to permeate freely while preventing the polymers from escaping. The sensing chamber is filled with a solution of a glucose-affinity polymer (the sensing solution), while the reference chamber contains a solution of a polymer that does not bind with glucose (the reference solution).

The transducing elements in the viscometric sensor are freestanding diaphragms that vibrate under the force exerted by an external alternating current (AC) magnetic field on Permalloy thin-film lines integrated on the diaphragms (**Figure 1A**).[12] The vibration of each diaphragm is measured via an embedded electrode, which forms a parallel-plate capacitive displacement transducer with another electrode lying on the substrate with air as the dielectric material. On the other hand, the transducing elements in the dielectric sensor are parallel-plate capacitive electrodes, one of which is perforated to allow diffusive transport of glucose molecules. This design eliminates moving mechanical structures, leading to improved reliability (**Figure 1B**). The gap of the perforated electrode transducer is filled with polymer solution, whose permittivity determines the capacitance between the electrodes. Binding of glucose with the affinity polymer induces a change in the viscosity or permittivity of the solution, which can be determined by measuring the diaphragm vibration using the capacitive displacement transducer, or the capacitance of the perforated electrode transducer. Differential measurements from such transducers within the sensing and reference modules allow accurate determination of glucose concentration while rejecting influences of fluctuations in environmental parameters.

The MEMS differential sensors use poly(N-hydroxyethyl acrylamide-ran-3-acrylamidophenylboronic acid) (PHEAA-*ran*-PAAPBA) as the sensing polymer. The synthesis and characterization of this polymer have been described in detail elsewhere.[24] Briefly, PHEAA-*ran*-PAAPBA is an amphiphilic copolymer composed of a hydrophobic glucose-sensitive component poly(acrylamidophenylboronic acid) (PAAPBA) and a hydrophilic, nonionic component poly(N-hydroxyethyl acrylamide) (PHEAA). The presence of PHEAA improves the overall water solubility of the copolymer and likely provides additional neighbor coordinating effects to enhance the glucose-binding specificity.[24] In an aqueous environment at physiological pH, glucose can bind reversibly to the phenylboronic acid moieties in the PAAPBA segments, resulting in strong cyclic boronate ester bonding and cross-linking of PHEAA-*ran*-PAAPBA. This changes the viscosity of the polymer solution as well as the polarization behavior of the polymer in an electrical field. On the other hand, a glucose-insensitive polymer poly(acrylamide) (PAA), whose solution viscosity and permittivity vary negligibly with the presence of glucose,[22,23] is used as a reference polymer.

Fabrication and Experimental Setup

The differential glucose sensors were fabricated using standard MEMS techniques, which include thin film deposition and patterning through photolithography and etching. The detailed fabrication processes are described elsewhere.[25–27] The resulting devices have

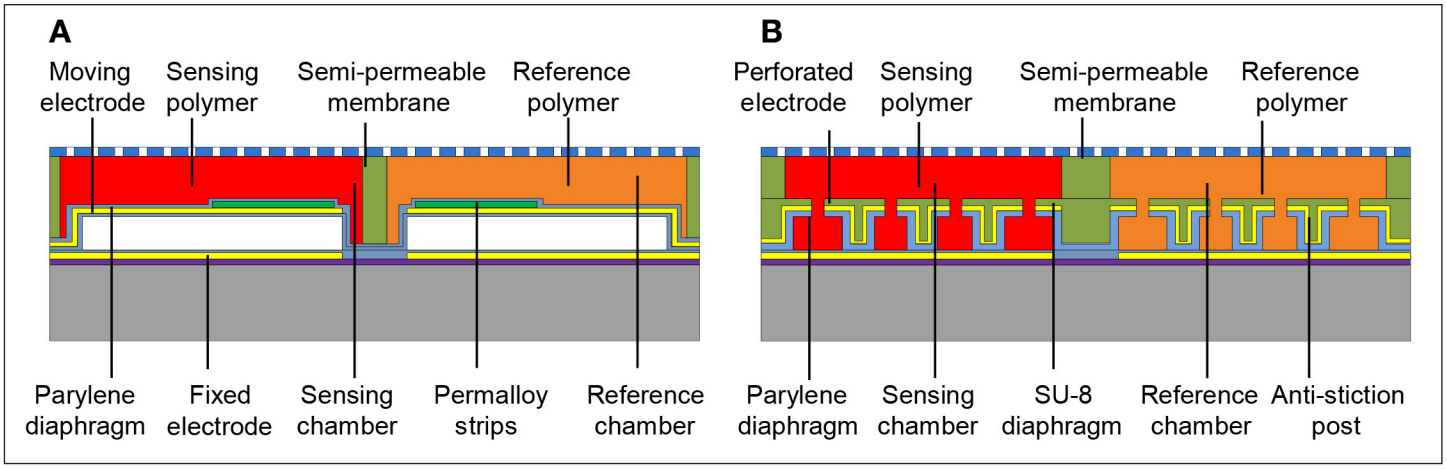

Figure 1. Schematics of the MEMS differential glucose sensors based on **(A)** viscosity and **(B)** permittivity detection.

5 × 7 and 5 × 10 mm^2 footprints and are connected via flexible electric cables to an external signal read-out unit that measures capacitance at a fixed frequency. The experimental setup (**Figure 2**) for both viscometric and dielectric sensors has been described previously.[26,27] In short, the experimental setup includes a capacitance digital converter, which provides an AC bias at 32 kHz to the moving or perforated electrodes and measures the charges on the bottom electrodes through a modulator. As a result, capacitance can be determined through the charging or discharging time of the sensor electrodes. The viscometric sensor additionally utilizes a spinning permanent magnet (within the dashed square in **Figure 2**) that periodically magnetizes the Permalloy strips on the diaphragms to provide a changing torque, resulting in the vibration of the moving electrodes.

Materials and Experimental Methods

Chemicals used in the experiments include PHEAA-*ran*-PAAPBA and PAA, which were synthesized in-house by free radical polymerization.[24] Phosphate-buffered saline (PBS), pH 7.4, was prepared by diluting a Ringer's stock solution (Nasco Inc.) with sterile water (Fisher Scientific) at a ratio of 1:9. The sensing polymer solution was prepared by dissolving 284 mg of PHEAA-*ran*-PAAPBA (molar ratio, PHEAA/PAAPBA = 20/1; molecule weight, 188,600) in PBS (6 ml), while the reference polymer solution was prepared by dissolving 142 mg of PAA (molecular weight, 0.6 × 10^6 to 9 × 10^6)[28] in PBS (6 ml) to achieve compatible viscosity as the sensing polymer solution.

Preliminary animal testing was conducted at the Columbia University Medical Center using 10-week-old C57BL/6J laboratory mice using a protocol approved by the Columbia University Institutional Animal Care and Use Committee. Under inhaled isoflurane (3–3.5%) in oxygen anesthesia, shaved skin was prepped with betadine and alcohol washes and a 1.5–2 cm incision caudal to the interscapular region was made, avoiding the interscapular brown adipose tissue depot. A hemostat was used to make a small pouch in which the sensor was placed. Blood glucose concentrations were manipulated by intraperitoneal (IP) administration of glucose (2 g/kg) followed by insulin (0.25 U/kg). Capillary blood glucose was monitored with a commercial glucose meter (Freestyle Lite, Abbott Diabetes Care) by tail nicking. One mouse was implanted with a viscometric sensor and three mice were implanted with the dielectric sensors. *In vitro* characterization prior to animal testing compared the behavior of single-module sensors that contain only the PHEAA-*ran*-PAAPBA polymer and differential sensors that use PAA as the reference polymer.[25] The differential sensors exhibited drastically improved temperature stability and negligibly small signal drift within the time frame of our animal testing. Thus monitoring of animal temperature was considered unnecessary and not conducted in the *in vivo* experiments. The mouse implanted with the viscometric sensor was first given an IP glucose injection (2 g/kg) to create hyperglycemia, followed by an IP injection of insulin (0.25 U/kg) causing a rapid decrease in blood glucose concentrations. In animal experiments using the dielectric sensor, blood glucose levels were first allowed to equilibrate for 1 h with no exogenous injections of glucose or insulin. The glucose levels of mice were then reduced by IP administration of short-acting insulin and afterward increased to induce hyperglycemia via glucose administration. The implanted glucose sensors continuously measured the glucose levels in ISF, while the commercial glucose meter was used to sample capillary (via tail) blood glucose concentrations at specified frequencies.

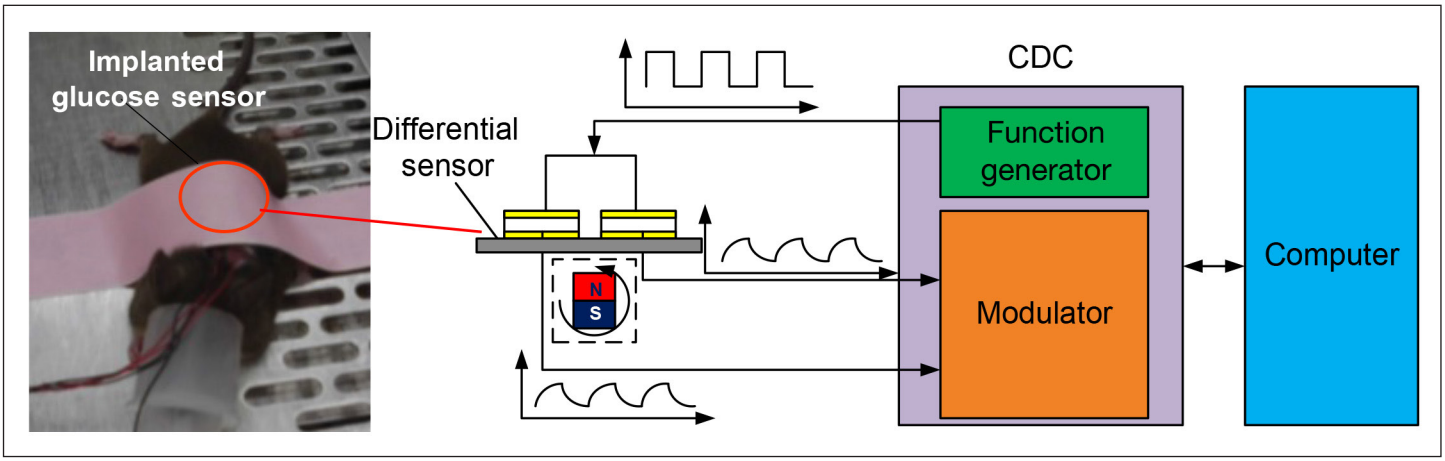

Figure 2. Experimental setup for testing the MEMS differential dielectric and viscometric sensors. CDC, capacitance digital converter.

Sensor Calibration

A data calibration method that uses glucose meter readings and accounts for time lags and nonlinearity during measurements was used to obtain the predicted glucose concentrations from the differential sensor capacitance. In this method, time lags between the differential capacitance and the glucose meter readings are attributed to exogenous mass transfer of glucose molecules between blood and ISF and endogenous glucose diffusion within the glucose sensors.[29] The dynamic glucose concentrations in ISF and blood are represented by a two-compartment model,[30] in which blood and ISF are considered as separate glucose-containing compartments that exchange glucose through capillary walls due to concentration gradients. As a result, ISF glucose values can be determined by the diffusion rate of glucose between blood and ISF and the rate of glucose uptake by subcutaneous tissue cells.[31] The concentration gradient in ISF glucose can be expressed as

$$dG_2/dt = -(k_{02} + k_{12})G_2 + k_{21}V_1/V_2G_1 \quad (1)$$

where G_1 and G_2 are blood and ISF glucose concentrations, respectively; k_{12} and k_{21} are the flux rates of forward or reverse glucose transport across the capillary; k_{02} is the glucose uptake into subcutaneous tissue; and V_1 and V_2 are the volumes of blood and ISF, respectively.

Existing CGM calibration methods for electrochemical sensors mostly use a simple linear equation $y = ax + b$ to represent the relation between CGM sensor outputs and blood glucose values. In this equation, x is a blood glucose value and y is a sensor output (e.g., electric current or voltage), while a and b are constants. Assuming $b = 0$ (zero current or voltage output from glucose sensors in a glucose-free environment), a one-point calibration (i.e., a reference glucose value from the glucose meter and a corresponding sensor output, which is also defined as a glucose concentration pair) can be used to determine a, the sensor sensitivity. If $b \neq 0$, a two-point calibration that is based on two glucose concentration pairs can be used to obtain a and b.[32]

However, affinity glucose sensors in general exhibit nonlinearity in response to glucose concentration changes.[27] Thus the relation between the differential sensor capacitance (C_{out}) and ISF glucose concentrations (G_2) may be represented by a quadratic equation as

$$G_2 = aC^2_{out} + bC_{out} + c \quad (2)$$

where a, b, and c are constants. Combining **Equations (1)** and **(2)** yields

$$G_1 = a_1C^2_{out} + a_2C_{out} + a_3C_{out}dC_{out}/dt + a_4dC_{out}/dt + a_5 \quad (3)$$

where a_1, a_2, a_3, a_4, and a_5 are constants, which reflect the glucose diffusion rates as well as time lags in the two-compartment model, and can be determined from least squares fitting using six blood reference values (G_1) from the glucose meter and the corresponding implanted sensor output values (C_{out}). Thus, for a given C_{out}, the predicted glucose value, denoted $\hat{G}_1$, can be obtained.

Results and Discussion

In vivo testing of the dielectric and viscometric glucose sensors were performed in sedated laboratory mice. In this section, we present the results associated with animal experiments, which include sensor initialization and time courses of implanted sensors in response to glucose and insulin administration. Clarke error grids are then presented to assess the clinical accuracy of the sensors.

Sensor Initialization

After implantation of the differential sensors in laboratory mice (**Figure 2**), an initialization period of approximately 8 to 30 min was required to allow the equilibrium of glucose and saline between the ISF and the polymer solutions that were originally free of glucose. A typical sensor response during this period is shown in **Figure 3**, in which the differential capacitance of a dielectric sensor was recorded over a period of approximately 8 min. The differential capacitance first decreased steadily by 0.04 pF following sensor implantation (time 0) to 0.68 pF at 2.5 min. This indicates a decrease in the permittivity of the PHEAA-*ran*-PAAPBA polymer solution due to affinity binding between the glucose and the glucose-free sensing polymer. The differential capacitance eventually stabilized at approximately 8 min, indicating the equilibrium of glucose and saline contents between microchambers and ISF.

In Vivo *Measurements*

Following sensor initialization, the time course of differential capacitance changes of the viscometric and dielectric sensors were obtained at varying glucose concentrations controlled by glucose and insulin administration. We first assessed interstitial glucose concentrations as represented by the measured differential capacitance of the viscometric sensor, compared with

blood glucose concentrations measured using the glucose meter. To facilitate visualization, we examined the changes in the measured differential capacitance calculated with respect to the differential capacitance value at the time of the first glucose meter reading (**Figure 4**). It can be seen that the trend in the output from viscometric sensor closely tracked that of the commercial glucose meter readings as the blood glucose levels varied over a measurement period of approximately 180 min. For the viscometric sensor, measured differential capacitance changed by approximately 0.2 pF from the time of glucose administration (time reset to t = 0 for data presentation purposes) to the time of insulin administration at t = 125 min, while the glucose meter reading increased from 193 to 500 mg/dl. Following insulin administration at t = 125 min, the blood glucose of the mouse rapidly dropped from 500 to 322 mg/dl at 130 min, which was accompanied by an increase of differential capacitance of approximately 0.03 pF. At approximately t = 100 min, the change in differential capacitance decreased while glucose concentrations maintained at the saturation level (500 mg/dl) of the glucose meter. As time further elapsed, the glucose meter reading gradually decreased by 51 to 271 mg/dl, while differential capacitance change decreased by 0.012 pF. Due to limitations in the early animal testing protocol in which insulin administration, conducted in a single mouse, was not sufficient to reduce large glucose concentration decreases, the measurement points were all in the hyperglycemic range. Despite the limitations, early preliminary data suggest that the MEMS differential viscometric sensor can correctly detect the trend in glucose concentration changes in an *in vivo* setting.

The time course of differential capacitance changes of the dielectric sensors was obtained using a similar procedure to that for the viscometric sensor, except that the glucose control protocol was improved, which involved insulin administration followed by glucose injection to enable testing in the hypoglycemic range. Results from one of the three mice tested are shown in **Figure 5**. It can be seen that the output from the dielectric sensor followed the trend in the readings of the commercial glucose meter over a measurement period of approximately 150 min. In addition, dielectric sensor output exhibited significantly less fluctuations as compared with viscometric sensors. This improved stability of the dielectric sensor could be attributed to the elimination of moving mechanical structures, which tend to be susceptible to external disturbances. Between t = 0 and 69 min (time reset to 0 upon completion of sensor initialization), the capillary blood glucose concentrations of the mouse reflected

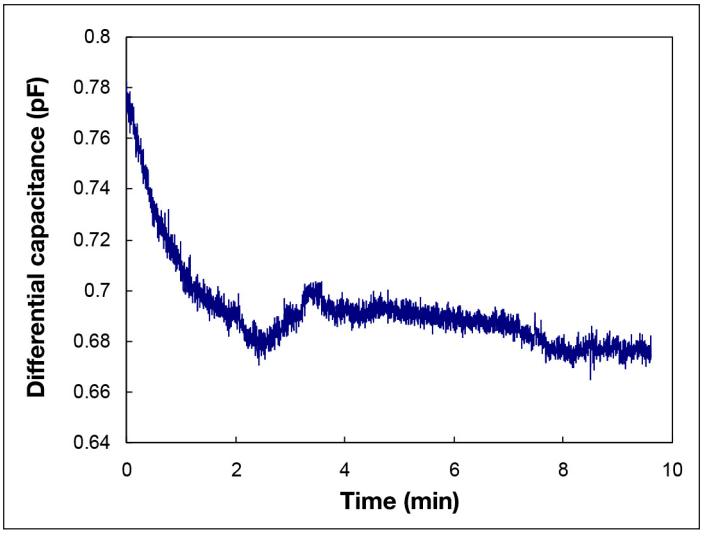

Figure 3. A typical differential capacitance change of the implanted sensor during the initialization period.

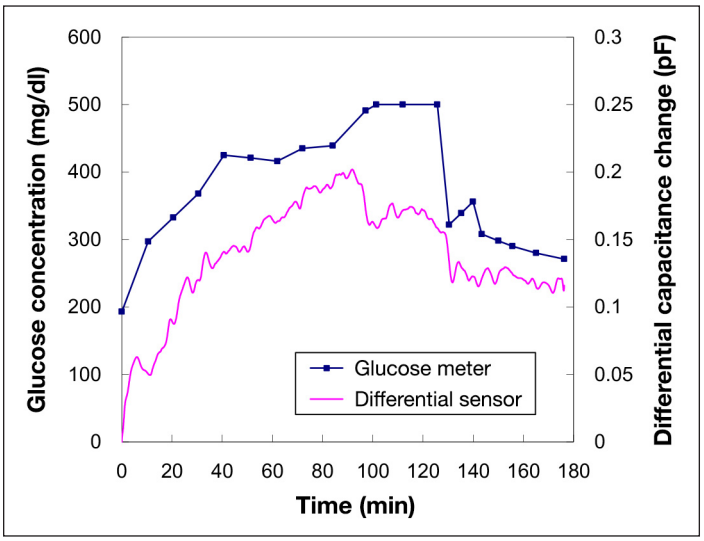

Figure 4. Animal testing results. Differential capacitance changes of a MEMS viscometric sensor as compared with readings from a commercial glucose meter.

solely endogenous glucose homeostasis. After insulin administration at 69 min, the glucose meter reading decreased consistently from 103 to 41 mg/dl (hypoglycemia), corresponding to a decrease of differential capacitance by 0.6 pF. In response to glucose administration at t = 101 min, the blood glucose concentration increased from 41 to 300 mg/dl, while differential capacitance increased by 1.15 pF. These results indicate that the differential dielectric sensor is capable of correctly tracking *in vivo* glucose concentration changes.

Time lags between the differential capacitance and the glucose meter readings during rapid glucose concentration changes existed for all mice tested and generally ranged

from 0 to 15 min. For the viscometric sensor, after glucose administration at 0 min, almost no time lag was observed until 101 min (**Figure 4**). Between 101 and 125 min, the glucose meter was out of range, and we were unable to assess time lag. After insulin administration at 125 min, a time lag of approximately 3 min was observed between the glucose meter reading and differential capacitance changes (**Figure 4**). In general, the time lag could be attributed to the times required by diffusive glucose transport across the capillary wall (physiological time lag) and within the microchamber of the device (device-dependent time lag). The reason for this apparently negligible time lag is not clear and needs to be investigated in future work. The physiological time lag is generally device-independent and can vary widely from 0 to 50 min, depending on the individual test subject.[33,34] As the device-dependent time lag was estimated to be 1.5 min,[27] this suggests that the observed time lag was probably due to comparable contributions from physiological and device-dependent time lags.

For the dielectric sensor whose animal testing results are shown in **Figure 5**, time lag between the device and glucose meter readings could not be resolved for the time period from 0 to 69 min when the mouse experienced endogenous glucose homeostasis. Upon insulin administration at 69 min, device output showed a time lag of approximately 6 min with respect to the glucose meter readings. The time lag increased to approximately 10 min after glucose administration at 101 min. The existence of different time lags during different stages of glucose concentration changes was also observed in the dielectric sensor testing in the other two animals[25] and was consistent with reported observations in the literature.[29,33–36] In addition, since the device-dependent time lag was estimated to be 2.6 min,[26] these observed time lag values suggest that the mouse had a significantly larger physiological time lag when compared with the animal used for the viscometric sensor testing.

Assessment of Microelectromechanical Systems Sensor Accuracy

Clinical accuracy of estimated ISF glucose concentration ($\hat{G}_1$) obtained from an implanted MEMS sensor as compared with reference blood glucose concentration (G_1) measured by a glucose meter can be assessed quantitatively by constructing Clarke error grids.[37] The Clarke error grid is a plot of the predicted ISF glucose concentrations with respect to reference glucose concentrations, partitioned into five zones (A, B, C, D, and E) that represent different levels of clinical accuracy. If a data point, consisting of a predicted concentration and the corresponding reference

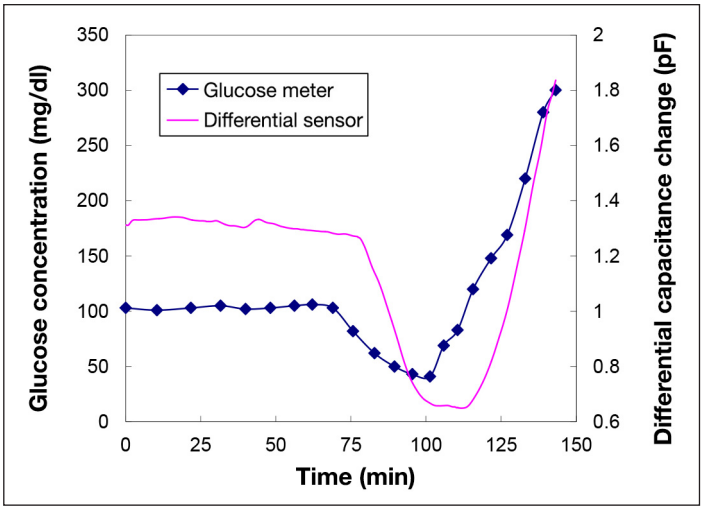

Figure 5. Animal testing results. Differential capacitance changes of a MEMS dielectric sensor as compared with readings from a commercial glucose meter.

concentration, falls into zone A, the prediction of the implanted sensor is considered clinically accurate. If the point lies within zone B, the predicted concentration is considered clinically acceptable. If the point falls in any of zones C, D, or E, it is considered as leading to overcorrection errors, dangerous failure, and erroneous treatment, reflecting a large discrepancy between the measurements from the implanted sensor and the glucose meter.

The Clarke error grids constructed from our *in vivo* testing are shown in **Figure 6** for the viscometric sensor (21 measurement points) and in **Figure 7** for the dielectric sensor (61 measurement points). The six reference values used for sensor calibration consist of two values in each of three time periods in which the glucose concentration stayed roughly at a constant, experienced a significant increase, and exhibited a significant decrease, respectively. These reference values were hence chosen at 20, 30, 61, 97, 135, and 143 min for the viscometric sensor (**Figure 4**) and at 33, 50, 83, 93, 104, and 126 min for the dielectric sensor (**Figure 5**). The corresponding device output (C_{out}) values at a reference time and at time 4 min prior were used to calculate the derivative dC_{out}/dt in **Equation (3)**. It can be seen that, for both sensors, all measurement points were located either in zone A or B and none in the other zones. Specifically, for the viscometric sensor, 95.3% of the measurement points fell in zone A and 4.7% in zone B. For the dielectric sensor, 83.6% of the points were in zone A and 16.4 % of points in zone B. These results suggested that all measurements from the implanted viscometric and dielectric sensors were clinically accurate or acceptable and that none of them

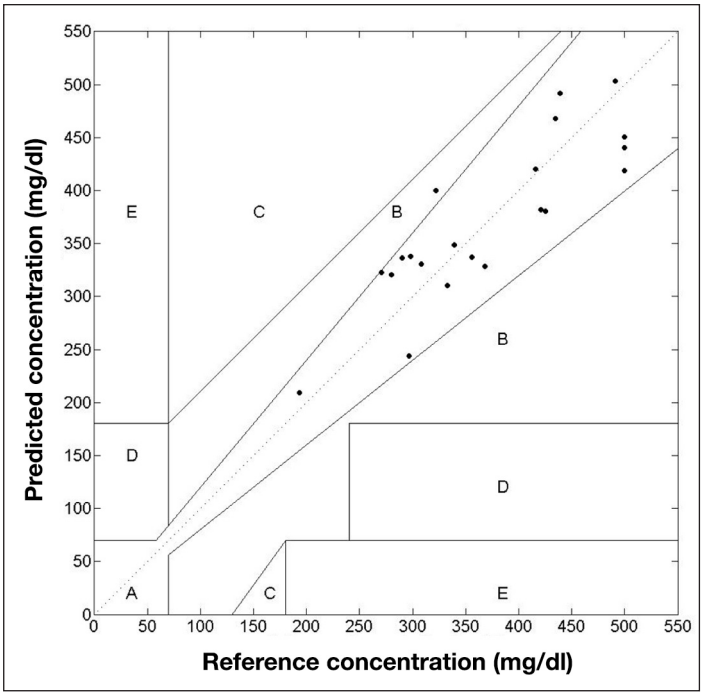

Figure 6. Clarke error grid for assessing the clinical accuracy of the ISF glucose concentrations predicted by the differential MEMS viscometric sensor with respect to reference blood glucose concentrations obtained from a glucose meter.

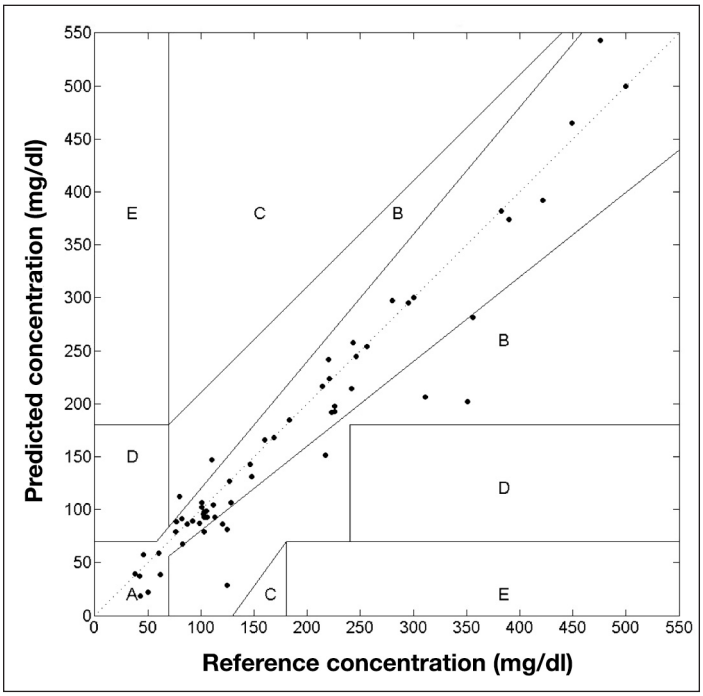

Figure 7. Clarke error grid for assessing the clinical accuracy of the ISF glucose concentrations predicted by the differential MEMS dielectric sensor with respect to reference blood glucose concentrations obtained from a glucose meter.

were clinically inaccurate or unacceptable. The dielectric sensors exhibited a better correlation to the glucose meter readings (correlation coefficient = 0.962) as compared with the viscometric sensor (correlation coefficient = 0.862), although the reason for this improvement is not yet clear and calls for further investigation. These results from Clarke error grid analysis suggest that the MEMS differential viscometric and dielectric sensors are potentially capable of accurately measuring ISF glucose concentrations when subcutaneously implanted for CGM.

Conclusion

In this article, we describe miniaturized MEMS differential glucose sensors based on detection of glucose-induced changes in the viscosity and permittivity changes of a glucose-specific polymer. Each type of sensor consists of a sensing module and a reference module that are respectively situated inside a microchamber filled with either the sensing polymer solution or a reference polymer solution. The viscometric sensor uses vibrational diaphragms that are excited by external AC magnetic field. The dielectric sensor features a pair of perforated electrodes embedded within parylene diaphragms, which allows the glucose to diffuse in and out of the gaps between the electrodes. Glucose concentrations can thus be determined from the difference in viscosity or permittivity between the sensing and reference polymer solutions via differential capacitive detection. The differential glucose sensors possess excellent stability and accuracy by effectively rejecting the common mode disturbances during the measurements.

The sensors were implanted into the subcutaneous tissue of laboratory mice and monitored the changes in glucose concentration in the ISF induced by exogenous glucose and insulin administration. For both types of sensors, the time courses of the implanted sensor output were consistent with those from the glucose meter readings. A calibration method was then used to correlate the implanted sensor output with the blood glucose concentration and allowed for analysis of clinical accuracy of the implanted sensors via Clarke error grids, yielding results that suggest that the ISF glucose measurements by the sensor are clinically accurate or acceptable. While testing in a larger number of animals is necessary in future research to obtain statistically significant data, this preliminary *in vivo* study offers evidence for the promise of subcutaneously implantable MEMS differential affinity sensors to ultimately enable long-term and stable CGM applications.

Funding:

This work was funded by the National Science Foundation Grant ECCS-0702101, the Columbia Diabetes and Endocrinology Research Center, the National Institutes of Health Grant DK63068-05, and the National Institutes of Health/National Institute of Diabetes and Digestive and Kidney Diseases Grant P30 DK63608-10.

References:

1. Yoo EH, Lee SY. Glucose biosensors: an overview of use in clinical practice. Sensors (Basel). 2010;10(5):4558–76.
2. Mastrototaro JJ. The minimed continuous glucose monitoring system. Diabetes Technol Ther. 2000;2 Suppl 1:S13–8.
3. Chia CW, Saudek CD. Glucose sensors: toward closed loop insulin delivery. Endocrinol Metab Clin North Am. 2004;33(1):175–95.
4. Weinstein R L, Schwartz S L, Brazg R L, Bugler J R, Peyser T A, McGarraugh G V. Accuracy of the 5-day freestyle navigator continuous glucose monitoring system: comparison with frequent laboratory reference measurements. Diabetes Care. 2007;30(5):1125–30.
5. Heller A. Implanted electrochemical glucose sensors for the management of diabetes. Annu Rev Biomed Eng. 1999;1:153–75.
6. Valdes TI, Moussy F. In vitro and in vivo degradation of glucose oxidase enzyme used for an implantable glucose biosensor. Diabetes Technol Ther. 2000;2(3):367–76.
7. Wisniewski N, Moussy F, Reichert WM. Fresenius J Anal Chem. 2000;366(6-7):611–21.
8. Amiss TJ, Sherman DB, Nycz CM, Andaluz SA, Pitner JB. Engineering and rapid selection of a low-affinity glucose/galactose-binding protein for a glucose biosensor. Protein Sci. 2007;16(11):2350–9.
9. Ballerstadt R, Schultz JS. A fluorescence affinity hollow fiber sensor for continuous transdermal glucose monitoring. Anal Chem. 2000;72(17):4185–92.
10. Liao KC, Hogen-Esch T, Richmond FJ, Marcu L, Clifton W, Loeb GE. Percutaneous fiber-optic sensor for chronic glucose monitoring *in vivo*. Biosens Bioelectron. 2008;23(10):1458–65.
11. Huang X, Li S, Schultz JS, Wang Q, Lin Q. A mems affinity glucose sensor using a biocompatible glucose-responsive polymer. Sens Act B. 2009;140(2):603–9.
12. Huang X, Li S, Schultz JS, Wang Q, Lin Q. A capacitive MEMS viscometric sensor for affinity detection of glucose. J Microelectromechanical Sys. 2009;18:1246–54.
13. Zhao Y, Li S, Davidson A, Yang B, Wang Q, Lin Q. A MEMS viscometric sensor for continuous glucose monitoring. J Micromech Microeng. 2007;17(12):2528–37.
14. Lei M, Baldi A, Nuxoll E, Siegel RA, Ziaie B. A hydrogel-based implantable micromachined transponder for wireless glucose measurement. Diabetes Technol Ther. 2006;8(1):112–22.
15. Labib M, Hedström M, Amin M, Mattiasson B. A novel competitive capacitive glucose biosensor based on concanavalin a-labeled nanogold colloids assembled on a polytyramine-modified gold electrode. Anal Chim Acta. 2010;659(1-2):194–200.
16. Huang X, Li S, Schultz JS, Wang Q, Lin Q. A dielectric affinity microbiosensor. Appl Phys Lett. 2010;96:033701–3.
17. Pan M, Guo X, Cai Q, Li G, Chen Y. A novel glucose sensor system with Au nanoparticles based on microdialysis and coenzymes for continuous glucose monitoring. Sens Actuators A. 2003;108(1-3):258–62.
18. Hsieh YC, Zahn JD. Glucose recovery in a microfluidic microdialysis biochip. Sens Actuators B Chem. 2005;107(2):649–56.
19. Zimmermann S, Fienbork D, Stoeber B, Flounders AW, Liepmann D. A microneedle-based glucose monitor: Fabricated on a wafer-level using in-device enzyme immobilization. Transducers. 2003;101:99–102.
20. Eun-Joo P, Werner J, Jaiswal D, Webb A G, Smith N B. Feasibility of a closed-loop controlled noninvasive ultrasonic glucose sensing and insulin delivery system. Ultrasonics Symposium. 2009;1749–52.
21. Paranjape M, Garra J, Brida S, Schneider T, White R, Currie J. A pdms dermal patch for non-intrusive transdermal glucose sensing. Sens Actuators A. 2003;104:195–204.
22. Himanshu AK, Bandyopadhayay SK, Bahuguna R, Ray DK, Sinha TP. Synthesis and dielectric studies of polyaniline-polyacrylamide conducting polymer composites. AIP Conf Proc. 2011;1349:204–5.
23. Shin S, Cho Y I. Temperature effect on the non-newtonian viscosity of an aqueous polyacrylamide solution. Int Comm Heat Mass Trans. 1993;20:831–44.
24. Li S, Davis EN, Huang X, Song B, Peltzman R, Sims DM, Lin Q, Wang Q. Synthesis and development of poly(n-hydroxyethyl acrylamide)-ran-3-acrylamidophenylboronic acid polymer fluid for potential application in affinity sensing of glucose. J Diabetes Sci Technol. 2011;5(5):1060–7.
25. Huang X. Miniaturized implantable affinity sensors for continuous glucose monitoring. Dissertation. New York: Columbia University; 2011.
26. Huang X, LeDuc C, Ravussin Y, Li S, Song B, Wang Q, Accili D, Leibel R, Lin Q. A MEMS differential dielectric sensor for continuous glucose monitoring. In: IEEE 25th International Conference on MEMS, 2012.
27. Huang X, Oxsher J, LeDuc C, Ravussin Y, Wang Q, Accili D, Leibel R, Lin Q. A MEMS differential affinity sensor for continuous glucose detection. In: 16th International on Solid-State Sensors, Actuators and Microsystems Conference (TRANSDUCERS), 2011.
28. Wu C, Quesada MA, Schneider DK, Farinato R, Studier FW, Chu B. Polyacrylamide solutions for DNA sequencing by capillary electrophoresis: Mesh sizes, separation and dispersion. Electrophoresis. 1996;17(6):1103–9.
29. Rebrin K, Steil GM, van Antwerp WP, Mastrototaro JJ. Subcutaneous glucose predicts plasma glucose independent of insulin: implications for continuous monitoring. Am J Physiol. 1999;277(3 Pt 1):E561–71.
30. Rebrin K, Steil GM. Can interstitial glucose assessment replace blood glucose measurements? Diabetes Technol Ther. 2000;2(3):461–72.
31. Cengiz E, Tamborlane WV. A tale of two compartments: Interstitial versus blood glucose monitoring. Diabetes Technol Ther. 2009;11 Suppl 1:S11–6.
32. Choleau C, Klein JC, Reach G, Aussedat B, Demaria-Pesce V, Wilson GS, Gifford R, Ward WK. Calibration of a subcutaneous amperometric glucose sensor. Part 1. Effect of measurement uncertainties on the determination of sensor sensitivity and background current. Biosens Bioelectron. 2002;17(8):641–6.
33. Keenan DB, Mastrototaro JJ, Voskanyan G, Steil GM. Delays in minimally invasive continuous glucose monitoring devices: a review of current technology. J Diabetes Sci Technol. 2009;3(5):1207–14.
34. Rebrin K, Steil GM. Can interstitial glucose assessment replace blood glucose measurements? Diabetes Technol Ther. 2000;2(3):461–72.
35. Kulcu E, Tamada JA, Reach G, Potts RO, Lesho MJ. Physiological differences between interstitial glucose and blood glucose measured in human subjects. Diabetes Care. 2003;26(8):2405–9.
36. Boyne MS, Silver DM, Kaplan J, Saudek CD. Timing of changes in interstitial and venous blood glucose measured with a continuous subcutaneous glucose sensor. 2003;52(11):2790–4.
37. Clarke WL, Cox D, Gonder-Frederick LA, Carter W, Pohl SL. Evaluating clinical accuracy of systems for self-monitoring of blood glucose. Diabetes Care. 1987;10(5):622–8.